Comparative Performance Analysis of Lead-Free Perovskites Solar Cells by Numerical Simulation

Shristy Srivastava
Central University of Jharkhand
Anand Kumar Singh
Central University of Jharkhand
Prashant Kumar
Central University of Jharkhand
Basudev Pradhan (basudev.pradhan@cuj.ac.in)
Central University of Jharkhand

Research Article

Keywords: Lead free perovskites, SCAPS-1D, Simulation, CsSnI3, efficiency

Posted Date: June 4th, 2021

DOI: https://doi.org/10.21203/rs.3.rs-583148/v1

Comparative Performance Analysis of Lead-Free Perovskites Solar Cells by Numerical Simulation

Shristy Srivastava[a], Anand Kumar Singh[a], Prashant Kumar[a], and Basudev Pradhan[a,b,*]

[a]*Department of Energy Engineering, Central University of Jharkhand, Brambe, Ranchi, Jharkhand, 835205, India*
[b]*Centre of Excellence (CoE) in Green and Efficient Energy Technology (GEET), Central University of Jharkhand, Brambe, Ranchi, Jharkhand, 835205, India*

**Corresponding author. E-mail address: basudev.pradhan@cuj.ac.in (B. Pradhan)*

Abstract

Research of lead-free perovskite based solar cells has gained speedy and growing attention with urgent intent to eliminate toxic lead in perovskite materials. The main purpose of this work is to supplement the research progress with comparative analysis of different lead-free perovskite based solar cells by numerical simulation method using solar cell capacitance simulator (SCAPS-1D) software. In this work, the device simulation is carried out in the *n-i-p* configuration of FTO/[6,6]-Phenyl-C61-butyric acidmethyl ester (PCBM) /Perovskite layer/ Poly[bis(4-phenyl)(2,4,6-trimethylphenyl)amine(PTAA)/Au using six different lead-free perovskite materials. The impact of different perovskite materials layers including hole and electron transport layer thickness, doping concentration on solar cell performances has thoroughly been investigated and optimized. $CsSnI_3$ based perovskite solar cell shows the highest power conversion efficiency of 28.97 % among all the lead-free perovskite based devices. This clearly indicates that it's possible to achieve high-performance lead-free perovskite solar cells experimentally at par with lead based perovskite solar cells in future research.

Keywords: Lead free perovskites, SCAPS-1D, Simulation, $CsSnI_3$, efficiency

1. INTRODUCTION

Perovskite solar cells have experienced a major leap in their power conversion efficiency (PCE) just over a decade due to their very simple manufacturing process, comparatively low processing cost, high absorption coefficient, low surface recombination rates and relatively high efficiency[1,2]. It has increased from 3.8% in 2009 to 25.5% till date in single-junction architectures, which is quite close enough to the crystalline silicon solar cells at 26.7%[3,4]. The hybrid organic-inorganic perovskites have opened new doors towards more efficient light harvesting materials. Owing to the property of tuneable frequency, these solar cells can be quite effective in absorbing different light frequencies by different layers which can lead to a boost in their efficiencies unlike the conventional solar cells. Despite this, lead based perovskites have two major challenges: a) poor stability which is being addressed by improved device engineering and encapsulation as well as incorporating the use of 2D perovskites, b) high toxicity that is raising a concern on an environmental level. Lead free perovskite materials, which are non-toxic and are also being looked upon as another alternative[5]. These lead free materials will be a preference in the solar cell market which will help in commercialization of perovskite solar cells if they do not compromise with the device performance. Ideally, Pb-free perovskites when used as light harvesting layers in solar cells, should have low toxicity, high optical absorption coefficients, low exciton-binding, narrow direct band gaps, high mobilities. Perovskites in the form of double perovskites, some Sn/Ge-based halides, and also some Bi/Sb-based halides with perovskite-like structure show fascinating properties and are low-toxicity materials. Up to 2020, the highest efficiency for Sn-based perovskites has been reported to have reached 13.24%[6].

In these Pb-free perovskite materials, comparatively only Sn-based PSCs have shown very promising performance. In Sn-based PSCs, certain factors like the poor air-stability caused due to quick oxidation of Sn^{2+} leading to increased recombination losses, small formation energy of vacancies, high intrinsic carrier density etc. leads to poor device performance as compared to their corresponding lead-based analogues. The anti-bonding coupling between Sn-5s and I-5p is comparatively weaker in $FASnI_3$ (FA = $CH(NH_2)_2$) than $CsSnI_3$ and $MASnI_3$ as a result of the larger ionic size of FA which is also the reason behind the increase in formation energies of Sn-vacancies[7,8]. According to the demonstration of Milot et al.

$FASnI_3$ exhibited high charge-carrier mobility in combination with very low Auger and strong radiative bimolecular recombination rate constants, which is similar to GaAs[9]. A study involving band gap engineering reported the PCE of 5.73% for Pb-free perovskite material of $CH_3NH_3SnI_{3-x}Br_x$ [10]. Lee et al. achieved a PCE of 4.8% by fabricating $FASnI_3$ combined with SnF_2−Pyrazine complex in order to slow down the crystallization process[11]. Kumar et al. worked on $CsSnI_3$ absorber layer based PSC incorporating vacancy modulation which showed a maximum power PCE of 2.02% and the experiment was carried out in nitrogen filled glove box due to material instability[12]. Zhao et al. got a maximum PCE of 8.12% for the $FA_{0.75}MA_{0.25}SnI_3$-based device and an open-circuit voltage of 0.61 V by optimizing the ratio of FA and MA cations[13]. Abdelaziz et al. used SCAPS software to study the impact of thickness, defect density, doping on the device performance of ($HC(NH_2)_2$–SnI_3– $FASnI_3$) based Perovskite solar cell. The optimized device performance obtained had a PCE of 14.03%, V_{OC} as 0.92 V, J_{SC} as 22.65 mA/cm^2 and FF of 67.74% [14]. Neol et al. fabricated a device with Pb-free $CH_3NH_3SnI_3$ as the absorber material in FTO/c-TiO_2/mp-TiO_2/$CH_3NH_3SnI_3$/Spiro-OMeTAD/Au device configuration that exhibited an efficiency of 6%[15]. It was observed that Sn^{2+} present in the lead- free light absorbing perovskite material transformed into Sn^{4+} under ambient atmosphere, in order to attain a more stable state. As a result, SnO_2 and methyl ammonium iodide (MAI) is formed as a result of the breaking of charge neutrality in the active perovskite. So, stability raises a concern when it comes to lead free Sn-based perovskites. However, the tin-based perovskites can use the same technologies to address the stability issues. When Pb-free perovskite candidates are concerned, which have already reached an efficiency of 13.24% by partial substitution of formamidinium cation with ethylammonium cation which also reduces the trap density by one Oder magnitude[6]. V_{OC} in the range of 0.8 to 1.00 V can be achieved if the Sn^{4+} oxidation issue is completely addressed and the photo carrier recombination rates are lowered down to the levels of the $APbI_3$ materials. This in turn could help in drastically improve the PCE beyond 15% and help them emerge as a viable lead-free contender in the near future[16].

In the field of lead free perovskites, several experiments are being performed to obtain information about their properties, possibilities and applications. The main concerns that are associated with Pb-free perovskites are (i) high-efficiency but poor stability (Sn^{2+}-based), or (ii) good stability but poor performance (Sn^{4+}/Sb/Bi-based etc.). A lead free perovskite that offers a good balance between the stability and performance needs to be found. An ideal Pb-free perovskite which has both good optical and electrical properties needs to be looked into.

Along with experiments, simulation also plays a vital role in analysing various properties of these materials and the corresponding performance parameters for various such materials. This work aids in studying the relation of the properties with the parameters, comparing multiple materials with the help of theoretical analysis by designing a device model. Here, a comparative study of various Pb-free perovskites on a similar configuration is done which helps us know about the distinguishing properties, their impacts on device performance and further work for achieving high efficiencies for Pb-free perovskites.

2. DEVICE ARCHITECURE AND SIMULATION METHODOLOGY

2.1. Device Architecture and modelling

In this simulation work, a comprehensive performance analysis has been studied on different lead free perovskite solar cell using the SCAPS-1D software. The undeniable feature of lead free perovskite material has gained importance in the past few years is its non-toxic nature unlike the lead based perovskite materials. The device configuration considered holds one of the most crucial aspects in the simulation being performed. In this work, the device simulation is carried out in *n-i-p* configuration of FTO/ [6,6]-Phenyl-C61-butyric acidmethyl ester (PCBM) /Perovskite layer/Poly[bis(4-phenyl)(2,4,6-trimethylphenyl)amine(PTAA)/Au, which is illustrated in Fig.1a. Here, PCBM has been used as an electron transport layer (ETL) and PTAA has been incorporated as a hole transport layer (HTL). Different lead free perovskite layer such as $FASnI_3$ (1.41eV), $CsSnI_3$ (1.3eV) Cs_2AgBiI_6 (1.6eV), $CsSnCl_3$ (1.52eV), Cs_2TiBr_6 (1.8eV) and $MASnI_3$ (1.35eV) are used as main absorber layer, which is sandwiched between ETL and HTL. Fluorine doped tin oxide FTO performs a dual function of serving as a front contact and as well as transparent conductive oxide through which light passes. Au acts as a back metal contact. In this study, the main focus has been laid on studying the behaviour of various lead free halide perovskites on the same device configuration. This will show the impact of the properties of each of the perovskites on the device performance and will also help in determining the lead free perovskite that performs the best on this particular configuration. Figure 1b shows the energy band diagram depicting the flow of charge carriers in the device constituting all the Pb-free perovskites along with the ETL, HTL and contacts. The basic materials information such as bandgap of the materials, thickness of various layers, doping concentration, mobility of electrons and holes, thermal velocities, electron affinity, dielectric permittivity, conduction band (CB) and valance band (VB) effective density of states are required for the simulation work which are also mentioned in the table 1.

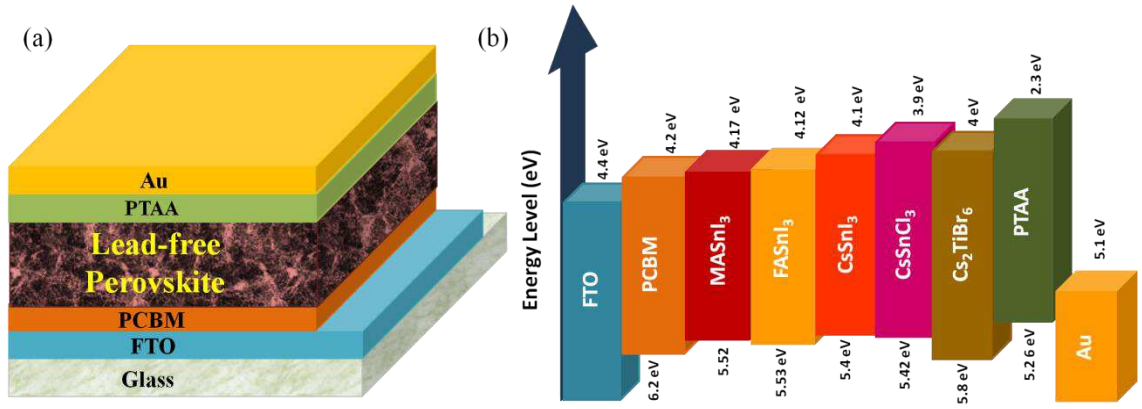

Fig. 1. (a) Schematic structure of the simulated PSCs, (b) Energy band diagram of different Pb-free perovskites with ETL and HTL

SCAPS-1D Simulation Methodology

The simulation and the calculations carried out in the SCAPS-1D software is mainly based on three basic equations namely the Poisson's equation, electron continuity equation and hole continuity equation respectively[17,18]. This software is a one dimensional solar cell simulation program that has been developed at the department of Electronics and Information Systems (ELIS) of the University of Gent, Belgium[19]. The device model that has been designed can perform up to a maximum of seven semiconductor layers and along with this, it provides the flexibility of grading and tuning different properties such as bandgap, electron affinity, defects, doping, interfacial properties etc. for each of the layers. The software is feasible for simulating different solar cell device structures from crystalline, amorphous to even organic and perovskite solar cells. The spectral condition under which the simulation has been performed is AM 1.5G 1 sun spectrum. The properties of each of ETL, HTL and the lead free perovskite layers have been varied to achieve an optimized result. The thickness and doping concentration has been varied within a feasible range in order to study the kind of plot obtained with the changing values. This makes it very simple and quite precise to obtain optimum values of each of the layers, which further helps in obtaining the optimized performing solar cell. This is done for all the lead free perovskites taken into consideration in this work which helps in analysing the performance and impact of the properties of each

material. The equations that play a significant role in the simulation study are inscribed below. Poisson's Equation for a semiconductor can be represented as follows:

$$\frac{d^2\psi(x)}{dx^2} = \frac{q}{\varepsilon}\,(n - p + N_A - N_D) \qquad \ldots\ldots (1)$$

Where, ε is the permittivity of the semiconductor, N_A represents the acceptor concentration, N_D is the donor concentration and ψ resembles the electrostatic potential.

Now, the electron and hole continuity equations for a semiconductor are given by:

Electron continuity equation:

$$\frac{\partial J_{n(x)}}{\partial x} - q\frac{\partial n}{\partial t} = +qR \qquad \ldots\ldots\ldots (2)$$

Hole continuity equation:

$$\frac{\partial J_{p(x)}}{\partial x} + q\frac{\partial p}{\partial t} = -qR \qquad \ldots\ldots\ldots (3)$$

In the above equations (2) and (3), J_n is the current density for electrons, J_P is symbolic of the current density for holes and R represents the rate of carrier recombination.

Another very important set of equations is the Drift-Diffusion current relations that are given by the continuity equations shown in (4) and (5). There are two ways in which current is conductor in a semiconductor. First and foremost, diffusion current which is produced due to the concentration gradient developed due to the difference in carrier concentration on either sides of the device. Secondly, and drift current that is build up due to the drift of minority charge carriers under the influence of electric field.

$$J_n = qn\mu_n E + qD_n\frac{\partial n}{\partial x} \qquad \ldots\ldots\ldots (4)$$

$$J_p = qp\mu_p E - qD_p\frac{\partial p}{\partial x} \qquad \ldots\ldots\ldots (5)$$

Where, D_p is the diffusion coefficient for holes and D_n is the diffusion coefficient for electrons. E represents the electric field, q is the quantity of charge, n and p represents the number of electrons and holes. μ_n and μ_p represents the mobility of electron and holes respectively. Other relations that govern the performance parameters are as follows:

For open circuit voltage:

$$V_{OC} = \frac{nkT}{q}\ln\left(\frac{J_{SC}}{J_S} + 1\right) \qquad \ldots\ldots\ldots (6)$$

Where, J_{SC} is the short circuit current density (or, light generated current), J_S is the reverse saturation current.

For short circuit current density:

$$J_{SC} = -J_L \quad \text{..... (7)}$$

Fill factor and efficiency is given by the relation:

$$FF = \frac{P_{max}}{J_{SC}\, V_{OC}} \quad \text{..... (8)}$$

$$\eta\,(PCE) = \frac{P_{max}}{P_{in}} = \frac{FF \times J_{SC} \times V_{OC}}{P_{in}} \quad \text{..... (9)}$$

For better device performance, light absorbing layer of solar cell has a major role. In this simulation different lead free perovskite materials will be used to find out best configuration to achieve higher performances. Major attention is given to optimise different parameters in a way through which we can get a clear insight of device performances. The table 1 shows the different layer parameters that have been used for this simulation process. Some values have been derived from the already published papers while the others have been optimized within the feasible limit after studying the impacts of different structural properties on the device performance.

Table1: main physical properties for various layers of lead free perovskite devices [14,18,20-27].

Material Properties	**PTAA**	**PCBM**	**FTO**	**$FASnI_3$**	**$CsSnI_3$**	**Cs_2BiAgI_6**	**$CsSnCl_3$**	**Cs_2TiBr_6**	**$MASnI_3$**
X (nm)	varied	varied	100	varied	Varied	varied	Varied	varied	varied
E_g (eV)	2.96	2.00	3.5	1.41	1.3	1.6	1.52	1.8	1.35
χ(eV)	2.3	3.9	4.0	3.52	3.6	3.9	3.9	3.9	4.17
ε_r	9	4	9	8.2	9.93	6.5	29.4	6.5	6.5
N_C (cm^{-3})	1×10^{21}	1×10^{21}	2.2×10^{18}	1×10^{18}	1×10^{19}	1×10^{19}	1×10^{19}	1×10^{19}	1×10^{18}
N_V (cm^{-3})	1×10^{21}	2×10^{20}	1.8×10^{19}	1×10^{18}	1×10^{18}	1×10^{19}	1×10^{19}	1×10^{19}	1×10^{19}
V_n (cm/s)	1×10^{7}	1×10^{7}	1×10^{7}	1×10^{7}	1×10^{7}	1×10^{7}	1×10^{7}	1×10^{7}	1×10^{7}
V_h (cm/s)	1×10^{7}	1×10^{7}	1×10^{7}	1×10^{7}	1×10^{7}	1×10^{7}	1×10^{7}	1×10^{7}	1×10^{7}
μ_n (cm^2/Vs)	1.00	1×10^{-2}	20	22	1.5×10^{3}	2	2	2	1.6
μ_h (cm^2/ Vs)	40	1×10^{-2}	10	22	5.85×10^{2}	2	2	2	1.6
N_D (cm^{-3})	-	varied	1×10^{17}	-	-	-	-	varied	-
N_A (cm^{-3})	varied	-	-	varied	Varied	varied	Varied	-	varied

3. RESULTS AND DISCUSSION

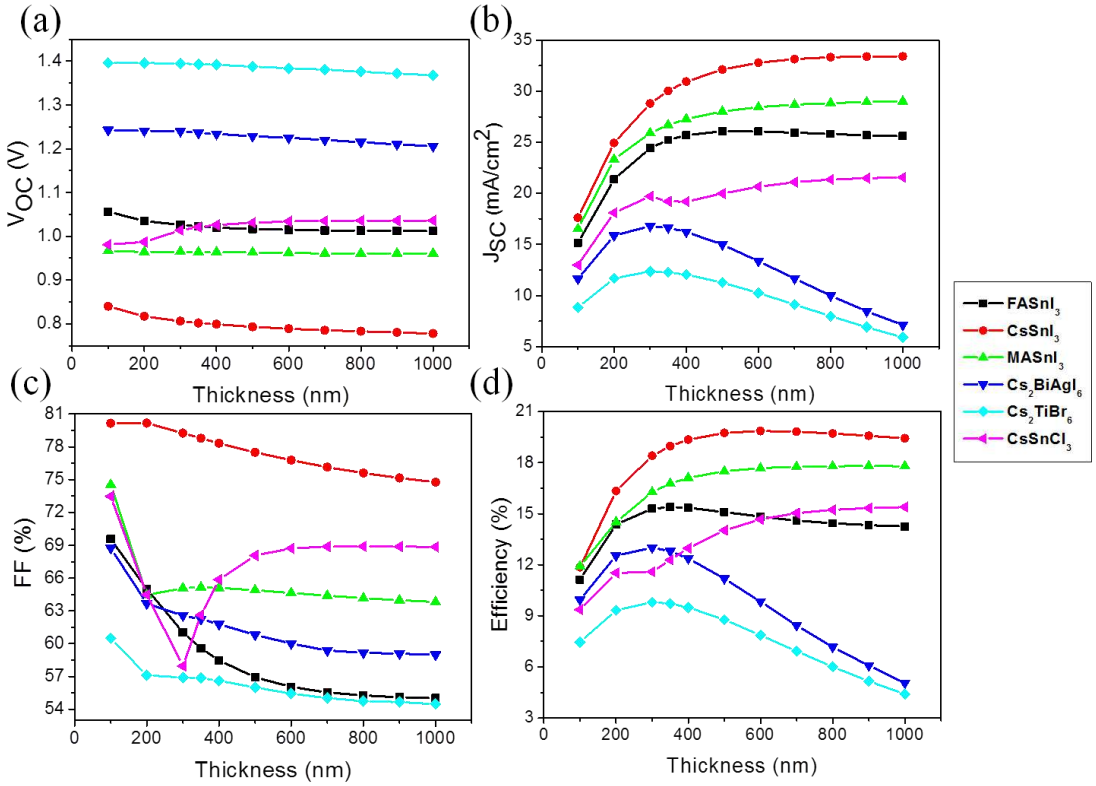

Fig. 2. Impact of thickness variation on the performance parameters of Pb-free perovskites

The numerical simulations of lead free perovskite solar cells were performed based on tabulated parameters collected from different theoretical and experimental papers. Different lead free perovskite materials have been used as an absorber layer in the device configuration of FTO/PCBM/Perovskite layer/PTAA/Au while keeping all the other parameters same except the light absorbing layer which has been varied between different lead free perovskites materials. Using this configuration, the device models have been simulated to obtain an optimized result for each case. To obtain optimized device performance, thickness and doping concentration of the active absorber layers were varied. Perovskite layer properties determine the device quality which is solely depend on the carrier diffusion lengths, charge carrier mobility values for both electrons and holes and carrier lifetime. The thickness of the perovskites has been varied to study the impact on the device performances. The thickness of the absorber layer has been varied in the range of 100 nm to 1000 nm keeping other parameters' including temperature is kept constant for the sake of comparative analysis. The

impact of thickness variation on the performance parameters of different Pb-free perovskites is shown in the Fig. 2. As the thickness increases, the open circuit voltage (V_{OC}) decreases or nearly remains the same for most of the perovskites shown in Fig. 2a. An uncommon behaviour is observed for $CsSnCl_3$ where the V_{OC} increases with thickness and then remains constant. The reason for this could be attributed to interfacial kinetics due to band energy mismatch. The nature of curves obtained for short circuit current density (J_{SC}) and efficiency (η) versus thickness is nearly same as depicted in Fig. 2b and 2d. As the thickness of absorber increases, the J_{SC} and η value increases, and reaches to the optimum value and decrease slowly with the increase of layer thickness for all perovskite materials, but the optimum thickness in which PCE reaches to highest value is different for different perovskite materials with which varies between 300 nm to 500 nm under this configuration. This trend could be explained by the fact that with the increase in active layer thickness more light absorption occurs in the device, that implies more charge carrier generation, and higher light generated current which ultimately leads to higher J_{SC} and efficiency[28]. Further increase in thickness may exceed the diffusion length of these materials, causing an increase in the recombination rate of charge carriers leading to increased saturation current, hence decreased $V_{OC,}$ and also J_{SC} which ultimately reduces efficiency. But, in some specific materials, such as $FASnI_3$, Cs_2BiAgI_6, and Cs_2TiBr_6 the values increase to a certain point and then decreases very fast with the increase of thickness. This may be because for these materials, after a certain point, the increase in absorber thickness leads to increased series resistance and back contact recombination hence leading to reduce J_{SC} and η. The fill factor plot (Fig. 2c) shows a decrease in value as the perovskite thickness increases and this could be explained by describing the *FF* dependency on perovskite layer thickness. Since, *FF* signifies how easily electron- hole pairs move through the device without recombination. With increased perovskite layer thickness, charge pathway resistance should increase leading to decrease in *FF*. On the other hand, internal recombination inside the lead-free perovskite material, occurred due to the short life time of electron (t_n) and hole (t_p) charge carriers, which do not permit adequate period for charge carrier to develop conduction band at lead-free perovskite material[20]. Certain abnormality of *FF* in case $CsSnCl_3$ with the increase of active layer thickness was also observed.

The dopant concentration of perovskite materials plays a very significant role in determining the electrical behaviour of the solar cell which has a major impact on the solar cell performance. The variation of doping for all lead-free perovskites has been plotted together

as a function of the solar cell performance parameters. The doping of the absorber layer has been varied in the range of 1×10^{14} to 5×10^{20} cm^{-3}. Rest all the properties are kept constant and the impact has been studied by comparing the behaviour of various materials. The figure 3 shows impact on different solar cell parameters due to the variation of doping concentration in different absorber materials. The open circuit voltage of all perovskite materials increase steadily with the increase of doping concentration as shown in Fig. 3a, reverse saturation current decrease with the increase of doping concentration, which leads to the increase in open circuit voltage[29,30]. On that hand built in potential (V_{bi}) as shown in the equation 10 is strongly dependent on the doping concentration.

$$V_{bi} = \frac{kT}{q} \ln \frac{N_A N_D}{n_i^2} \qquad (10)$$

where k is Boltzmann constant, T is temperature, q is the electron charge, n_i is intrinsic concentration, N_D is donor doping concentration and N_A is acceptor doping concentration. As the doping concentration increases the V_{bi} also increases which get reflected in $V_{OC.}$ The maximum V_{OC} is observed for Cs_2TiBr_6 (1.8eV) based device where as the lowest for $CsSnI_3$ (1.3eV) based device, other perovskites following the trend which is adequate because open circuit voltage is increasing with the increase in bandgap. The short circuit current densities of all the Pb-free perovskites decrease with the increase in doping as shown in Fig. 3b. Lower doping concentration serves for higher carrier collection due to a wider depletion region, increased doping levels leads to narrow charge collection region, hence, reduced J_{SC} at higher doping. The materials with higher band gaps have lower J_{SC} values and vice versa V_{OC} curve trend. The fill factor for most of the perovskites is seen to first decrease and then increases with the increase in doping values after which it remains almost constant, while a continuous increase in FF is observed for $FASnI_3$ and $CsSnI_3$ as shown in the Fig. 3c. The efficiency of most materials are seen to increase with increase in doping values while a decrease in η is observed in $MASnI_3$ and Cs_2TiBr_6 while for Cs_2BiAgI_6, initially it decreases and then increases slowly as shown in Fig. 3d. The nature obtained in this case is highly dependent on the behaviour each material reflects in the previous three performance parameters, hence, decrease in η of $MASnI_3$ and Cs_2TiBr_6 due to decrease in FF and J_{SC}. The explanation for such nature of FF and η could be due to decreased resistance with easy charge carrier pathway because of increased doping concentration.

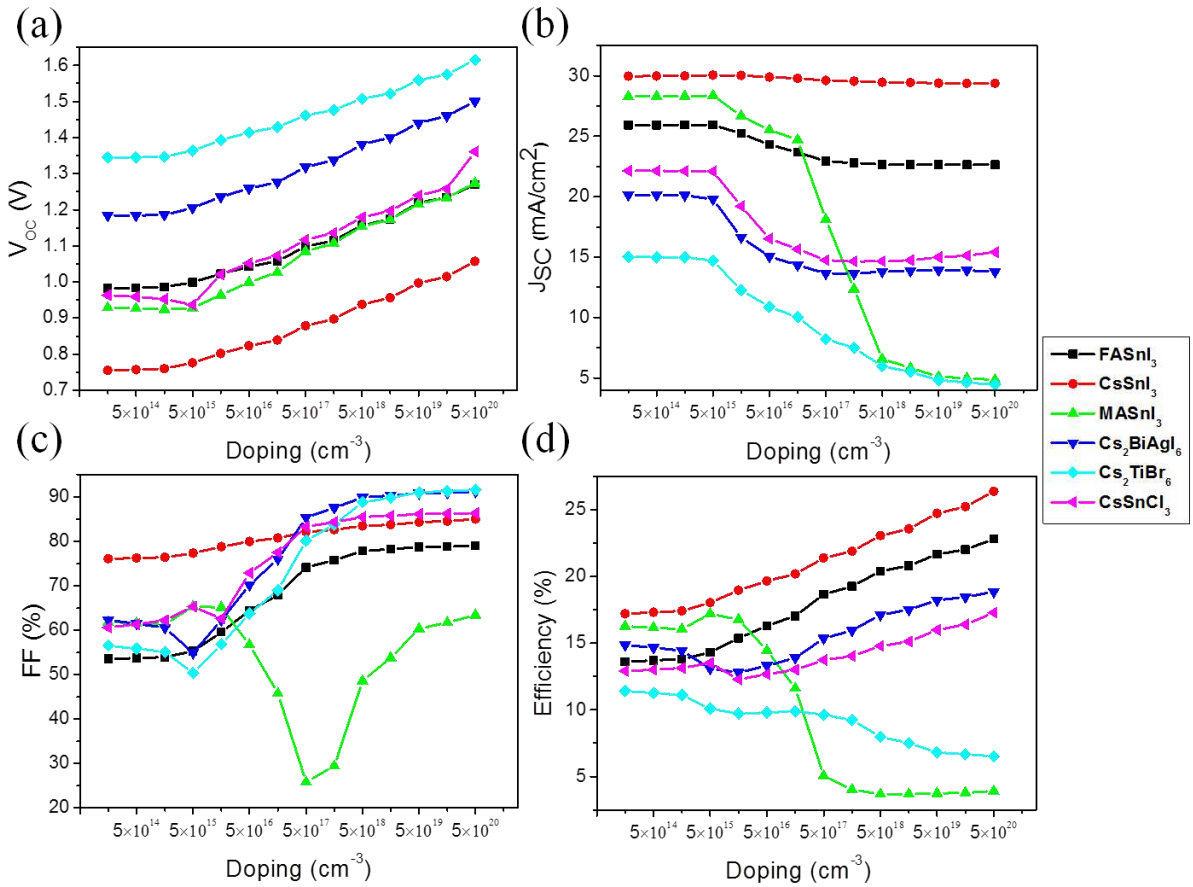

Fig. 3. Impact of doping variation on the performance parameters of Pb-free perovskites

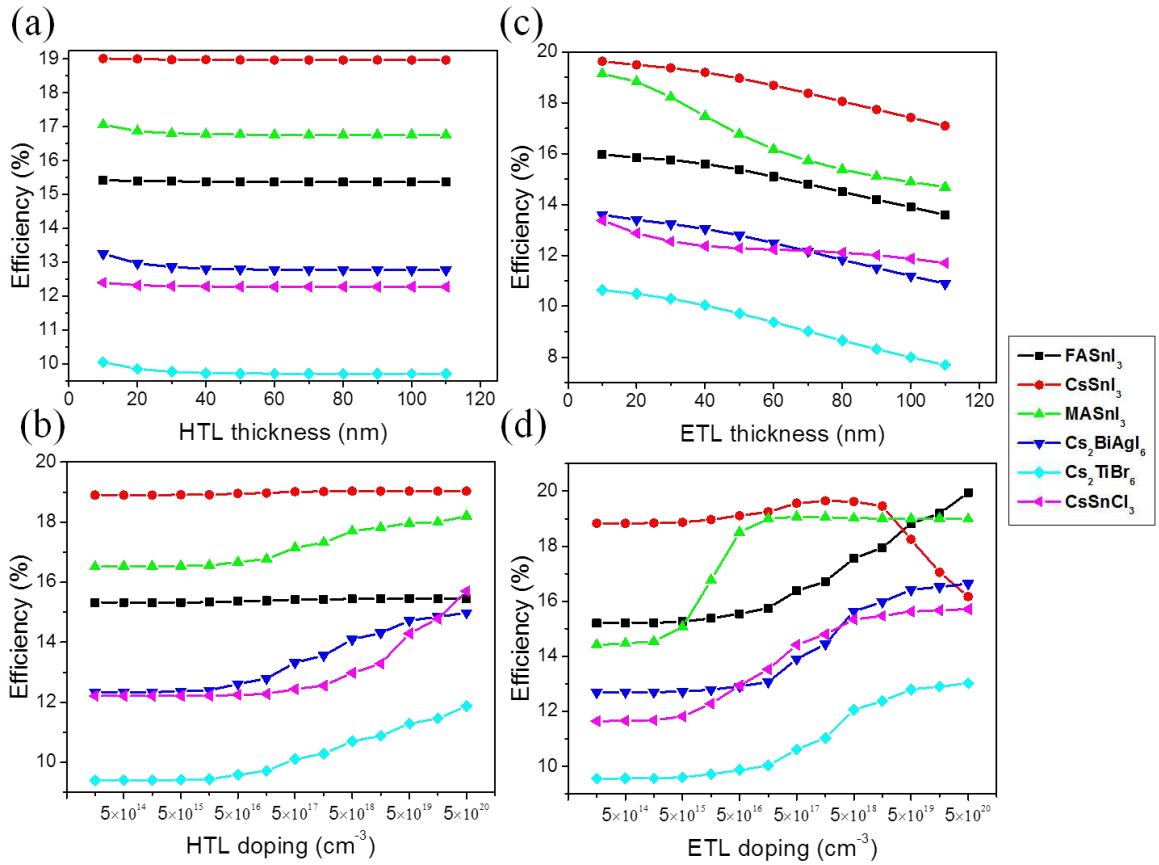

Fig. 4. Impact of doping and thickness variation of ETL, HTL on PSC performance

The variation in doping and thickness of the HTL layer i.e. PTAA has very negligible impact on the performance parameters of all the perovskites. As the figure 4a suggests, initially η decreases negligibly with the increase in HTL thickness and later it becomes constant for all perovskite based devices suggesting no major impact of HTL thickness on device PCE. Contrary to it a slight increase in the efficiency is observed as the HTL doping increases whereas, the value remain nearly constant in case of $FASnI_3$ and $CsSnI_3$ based devices as shown in Fig.4b. Electron transport layer aids in modifying the interface, controlling the charge recombination rates and also aligning the interfacial energy levels. The efficiency of all perovskite based devices decreases with the increase of ETL layer thickness which is shown in the Fig. 4c. On the other hand, Fig. 4d shows efficiency slowly increases with increase of the ETL doping. A continuous increase in the efficiency values are observed with the increase in doping of ETL, except for $CsSnI_3$ which after 10^{19} cm^{-3} doping value experiences a decrease in efficiency whereas in case of $MaSnI_3$ efficiency remain constant

after 10^{17} cm^{-3} doping concentration. Over all the efficiency increases slowly with the increase of HTL and ETL doping for most of the perovskites and become constant. As the donor concentration increases the conductivity also increases which reduces device J_{SC} and it maintains a constant value. After the certain limit of donor concentration the solar cell performance parameters remains unchanged due to Moss-Burstein effect[31]. Increase in doping of HTM and ETM layers also enhances the interface electric field between the HTL and ETL, this increased electric potential used to separate the excitons with less recombination rate and the performance of the device is increased. Alternatively, moderate doping is also needed whereas heavy doping leads to increased recombination and the perovskite semi-conductive nature changes to metallic which obstructs the carrier transport mechanism[32].

The *J-V* characteristics and quantum efficiency curve in light conditions for various lead-free perovskite materials have been plotted under optimized conditions as shown in the figure 5a and 5b respectively. All the devices show very good *J-V* characteristics. $CsSnI_3$ having the lowest band gap has the broadest absorption spectrum and Cs_2TiBr_6 having the narrowest of all, rest materials falling in order. However, as per the QE curves obtained, the working devices with best QE is $CsSnCl_3$, $MASnI_3$ and $CsSnI_3$ respectively as their active layers, with minimum energy losses with maximum QE values obtained at 98.4%, 99.7% and 96.67% respectively. The QE values at the low wavelength region for these materials suggest that the electrons due to the high energy photons are efficiently generated and collected. On the other hand it also reflected that the front surface is well passivated. In the high wavelength region, a high QE is observed in $MASnI_3$ and $CsSnI_3$ based device, which ultimately leads to higher short circuit current. The table 2 represents the performance parameters obtained for six different Pb-free perovskites based solar cells, when simulated under AM 1.5G 1sun spec, 300K temperature and all other working conditions same. Among all the devices, $FASnI_3$ shows highest V_{OC} of 1.277 V, whereas $MASnI_3$ shows lowest V_{OC} of 0.921 V. The device with $MASnI_3$ shows highest short circuit current density of 31.85mA/cm^2. $CsSnI_3$ and $FASnI_3$ based device shows higher *FF* as compare other devices. Figure 5c shows the energy band diagram of $CsSnI_3$ based perovskite with PTAA as hole transport layer and PCBM as electron transport layer from the SCAPS-1D software. Overall $CsSnI_3$ based device shows highest power conversion efficiency of 28.97 % with V_{OC} of 1.048 V, J_{SC} of 31.85mA/cm^2 and *FF* of 87.66% among the other perovskite based solar cells, which is so far the highest reported value in this configuration by any simulation method. The high performance of $CsSnI_3$ based solar cell would be due to small optical bandgap of perovskite material

combined with high optical absorption coefficient and low exciton binding energy. At the same time it also shows high electron dimensionality[33], relatively high intrinsic or thermodynamic stability[34]. It was also observed from the generation and recombination depth profile of the charge carrier that the charge carrier generation is high at PCBM and perovskite interface and carrier recombination is less whereas in the PTAA and perovskite interface, generation is less and carrier recombination is high. Therefore, from this simulation work, it is clear that $CsSnI_3$ based lead free perovskite solar cell definite be best alternate to the lead based perovskite solar cells.

Table 2: Performance parameters for optimized devices with various Pb-free perovskites

Pb- free Perovskite	**V_{OC} (V)**	**J_{SC} (mA/cm^2)**	**FF (%)**	**Efficiency (%)**
$FASnI_3$	1.277	22.40	86.36	24.70
$CsSnCl_3$	0.959	25.92	74.31	18.47
$MASnI_3$	0.921	31.85	77.81	22.82
Cs_2BiAgI_6	1.087	19.94	74.87	16.23
Cs_2TiBr_6	1.313	11.81	79.40	12.31
$CsSnI_3$	1.048	31.53	87.66	28.97

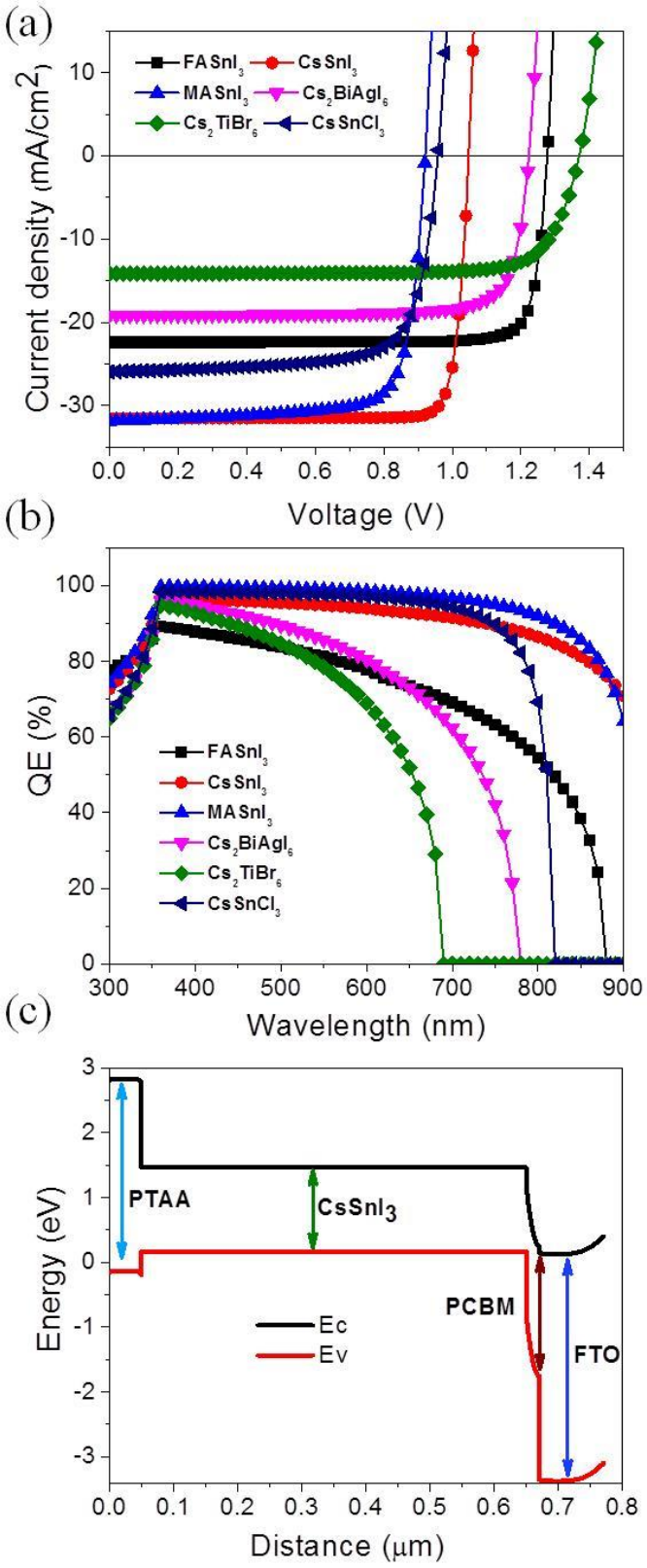

Fig. 5. (a) *J-V* characteristics, and (b) corresponding QE spectra of PSCs with different Pb-free perovskites. (c) Energy band structure diagram of the $CsSnI_3$ based perovskite solar cell.

4. CONCLUSION

In summary, comprehensive performance analysis of different lead-free perovskite based solar cells has been investigated by numerical simulation on SCAPS-1D. Detail comparative study has been performed to study the impact of different perovskite material properties, doping, thickness, and their impact on the PCE on the same device configuration having HTL as PTAA and ETL as PCBM. We have optimized different properties like doping density, the thickness of active materials as well as hole and electron transport layers for the further improvement of the device performance. Among all the lead-free perovskite based devices, $CsSnI_3$ based device shows the highest power conversion efficiency of 28.97 % with V_{OC} of 1.048 V, J_{SC} of 31.85mA/cm^2, and *FF* of 87.66%. So based on our simulation study, it is clear that lead-free perovskite based solar cells definitely guide the scientific community for further exploration towards experimental realization in lead-free perovskite based solar cells in the future.

Acknowledgement

BP would like to thank to Department of Science and Technology (Project No. -SB/FTP/PS-148/2013, SR/S2/RJN-55/2012, and DST/TM/CERI/C199) for financial support. The authors are also grateful to Ministry of Human Resources and Development (MHRD) for their financial support (project No. F.No. 5-5/2014-TS.Vll).

References

1 Correa-Baena, J.-P. *et al.* The rapid evolution of highly efficient perovskite solar cells. *Energy Environ. Sci.* **10**, 710-727 (2017).
2 Correa-Baena, J.-P. *et al.* Promises and challenges of perovskite solar cells. *Science* **358**, 739-744 (2017).
3 Kojima, A., Teshima, K., Shirai, Y. & Miyasaka, T. Organometal halide perovskites as visible-light sensitizers for photovoltaic cells. *J. Am. Chem. Soc.* **131**, 6050-6051 (2009).
4 https://www.nrel.gov/pv/cell-efficiency.html," can be found under https://www.nrel.gov/pv/cell-efficiency.html.
5 Jena, A. K., Kulkarni, A. & Miyasaka, T. Halide perovskite photovoltaics: background, status, and future prospects. *Chem. Rev.* **119**, 3036-3103 (2019).
6 Nishimura, K. *et al.* Lead-free tin-halide perovskite solar cells with 13% efficiency. *Nano Energy* **74**, 104858 (2020).

7 Shi, T. *et al.* Effects of organic cations on the defect physics of tin halide perovskites. *Journal of Materials Chemistry A* **5**, 15124-15129 (2017).
8 Gupta, S., Cahen, D. & Hodes, G. How SnF2 impacts the material properties of lead-free tin perovskites. *J. Phys. Chem. C* **122**, 13926-13936 (2018).
9 Milot, R. L. *et al.* Radiative monomolecular recombination boosts amplified spontaneous emission in HC (NH2) 2SnI3 perovskite films. *The journal of physical chemistry letters* **7**, 4178-4184 (2016).
10 Hao, F., Stoumpos, C. C., Cao, D. H., Chang, R. P. & Kanatzidis, M. G. Lead-free solid-state organic–inorganic halide perovskite solar cells. *Nature photonics* **8**, 489-494 (2014).
11 Lee, S. J. *et al.* Fabrication of efficient formamidinium tin iodide perovskite solar cells through SnF2–pyrazine complex. *J. Am. Chem. Soc.* **138**, 3974-3977 (2016).
12 Kumar, M. H. *et al.* Lead-free halide perovskite solar cells with high photocurrents realized through vacancy modulation. *Adv. Mater.* **26**, 7122-7127 (2014).
13 Zhao, Z. *et al.* Mixed-organic-cation tin iodide for lead-free perovskite solar cells with an efficiency of 8.12%. *Adv. Sci.* **4**, 1700204 (2017).
14 Abdelaziz, S., Zekry, A., Shaker, A. & Abouelatta, M. Investigating the performance of formamidinium tin-based perovskite solar cell by SCAPS device simulation. *Opt. Mater.* **101**, 109738 (2020).
15 Noel, N. K. *et al.* Lead-free organic–inorganic tin halide perovskites for photovoltaic applications. *Energy Environ. Sci.* **7**, 3061-3068 (2014).
16 Ke, W. & Kanatzidis, M. G. Prospects for low-toxicity lead-free perovskite solar cells. *Nat. Commun.* **10**, 1-4 (2019).
17 Raoui, Y. *et al.* Performance analysis of MAPbI3 based perovskite solar cells employing diverse charge selective contacts: Simulation study. *Solar Energy* **193**, 948-955 (2019).
18 Duan, Q. *et al.* Design of hole-transport-material free CH3NH3PbI3/CsSnI3 all-perovskite heterojunction efficient solar cells by device simulation. *Solar Energy* **201**, 555-560 (2020).
19 Burgelman, M., Nollet, P. & Degrave, S. Modelling polycrystalline semiconductor solar cells. *Thin Solid Films* **361**, 527-532 (2000).
20 Kumar, M., Raj, A., Kumar, A. & Anshul, A. An optimized lead-free formamidinium Sn-based perovskite solar cell design for high power conversion efficiency by SCAPS simulation. *Opt. Mater.* **108**, 110213 (2020).
21 Smith, B. Efficient Lead-Free Perovskite Solar Cell. (2018).
22 Owolabi, J. A., Onimisi, M. Y., Ukwenya, J. A., Bature, A. B. & Ushiekpan, U. R. Investigating the Effect of ZnSe (ETM) and Cu2O (HTM) on Absorber Layer on the Performance of Pervoskite Solar Cell Using SCAPS-1D. *Am J Phys Appl* **8**, 1 (2020).
23 Coulibaly, A. B., Oyedele, S. O. & Aka, B. Comparative study of lead-free perovskite solar cells using different hole transporter materials. *Modeling and Numerical Simulation of Material Science* **9**, 97-107 (2019).
24 Madan, J., Pandey, R. & Sharma, R. Device simulation of 17.3% efficient lead-free all-perovskite tandem solar cell. *Solar Energy* **197**, 212-221 (2020).
25 Li, S. *et al.* The investigation of inverted pin planar perovskite solar cells based on FASnI3 films. *Sol. Energy Mater. Sol. Cells* **199**, 75-82 (2019).

26 Khattak, Y. H., Baig, F., Shuja, A., Beg, S. & Soucase, B. M. Numerical analysis guidelines for the design of efficient novel nip structures for perovskite solar cell. *Solar Energy* **207**, 579-591 (2020).
27 Singh, A. K., Srivastava, S., Mahapatra, A., Baral, J. K. & Pradhan, B. Performance optimization of lead free-MASnI3 based solar cell with 27% efficiency by numerical simulation. *Opt. Mater.* **117**, 111193 (2021).
28 Koh, T. M. *et al.* Formamidinium tin-based perovskite with low E g for photovoltaic applications. *Journal of Materials Chemistry A* **3**, 14996-15000 (2015).
29 Lin, L. *et al.* Boosting efficiency up to 25% for HTL-free carbon-based perovskite solar cells by gradient doping using SCAPS simulation. *Solar Energy* **215**, 328-334 (2021).
30 Maram, D. K., Haghighi, M., Shekoofa, O., Habibiyan, H. & Ghafoorifard, H. A modeling study on utilizing ultra-thin inorganic HTLs in inverted p–n homojunction perovskite solar cells. *Solar Energy* **213**, 1-12 (2021).
31 Trukhanov, V., Bruevich, V. & Paraschuk, D. Y. Effect of doping on performance of organic solar cells. *Physical Review B* **84**, 205318 (2011).
32 Stoumpos, C. C., Malliakas, C. D. & Kanatzidis, M. G. Semiconducting tin and lead iodide perovskites with organic cations: phase transitions, high mobilities, and near-infrared photoluminescent properties. *Inorganic chemistry* **52**, 9019-9038 (2013).
33 Xiao, Z., Song, Z. & Yan, Y. From Lead halide Perovskites to Lead-free metal halide Perovskites and Perovskite derivatives. *Adv. Mater.* **31**, 1803792 (2019).
34 Zhou, Y. & Zhao, Y. Chemical stability and instability of inorganic halide perovskites. *Energy Environ. Sci.* **12**, 1495-1511 (2019).

Figures

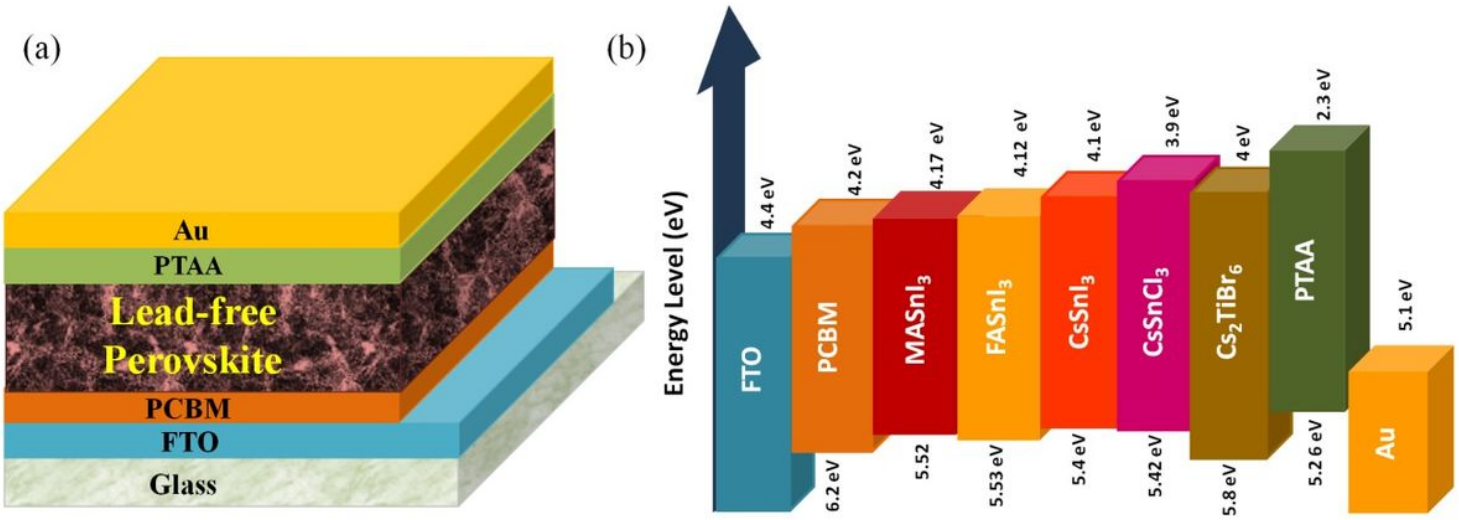

Figure 1

(a) Schematic structure of the simulated PSCs, (b) Energy band diagram of different Pb-free perovskites with ETL and HTL

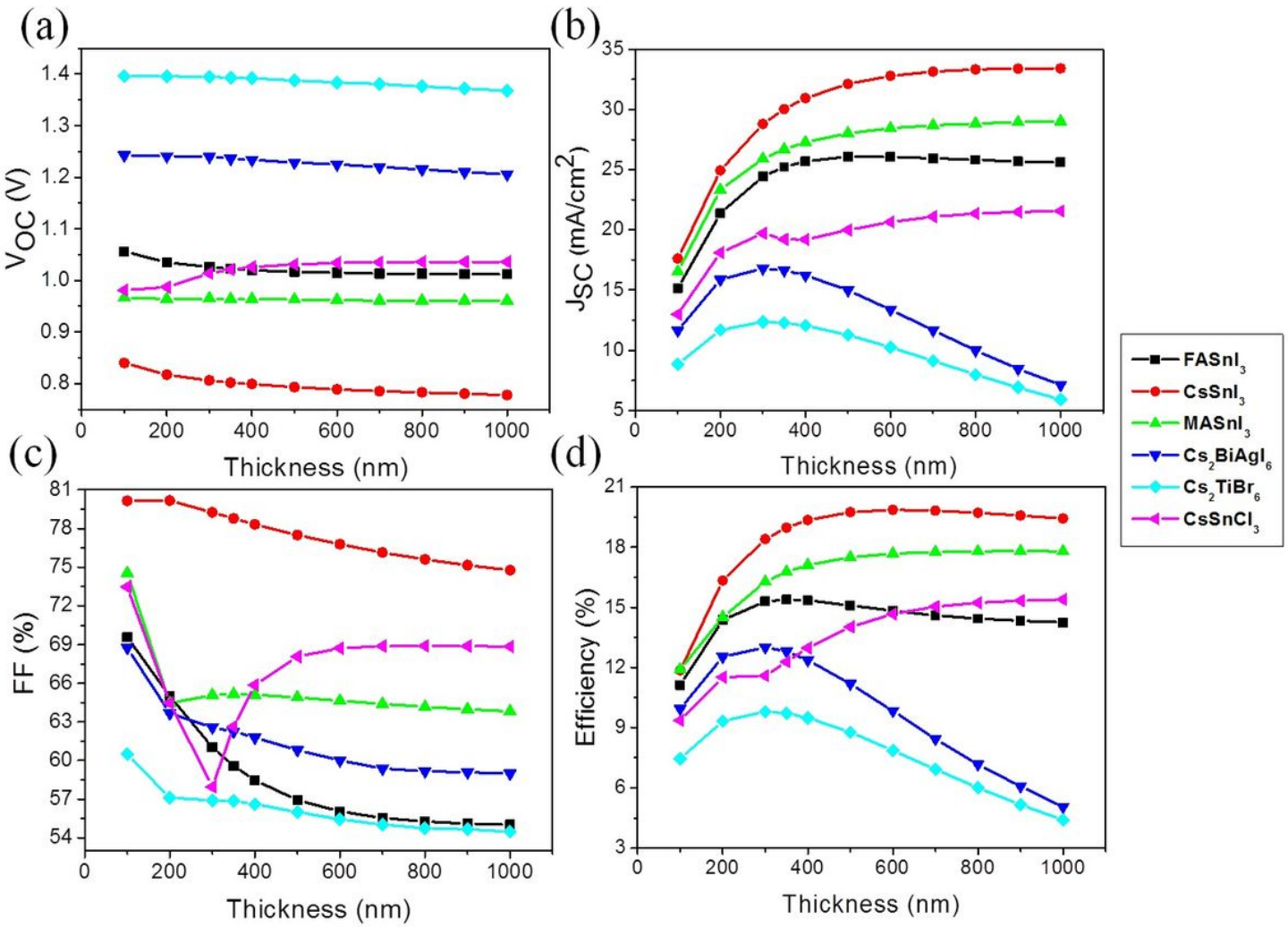

Figure 2

Impact of thickness variation on the performance parameters of Pb-free perovskites

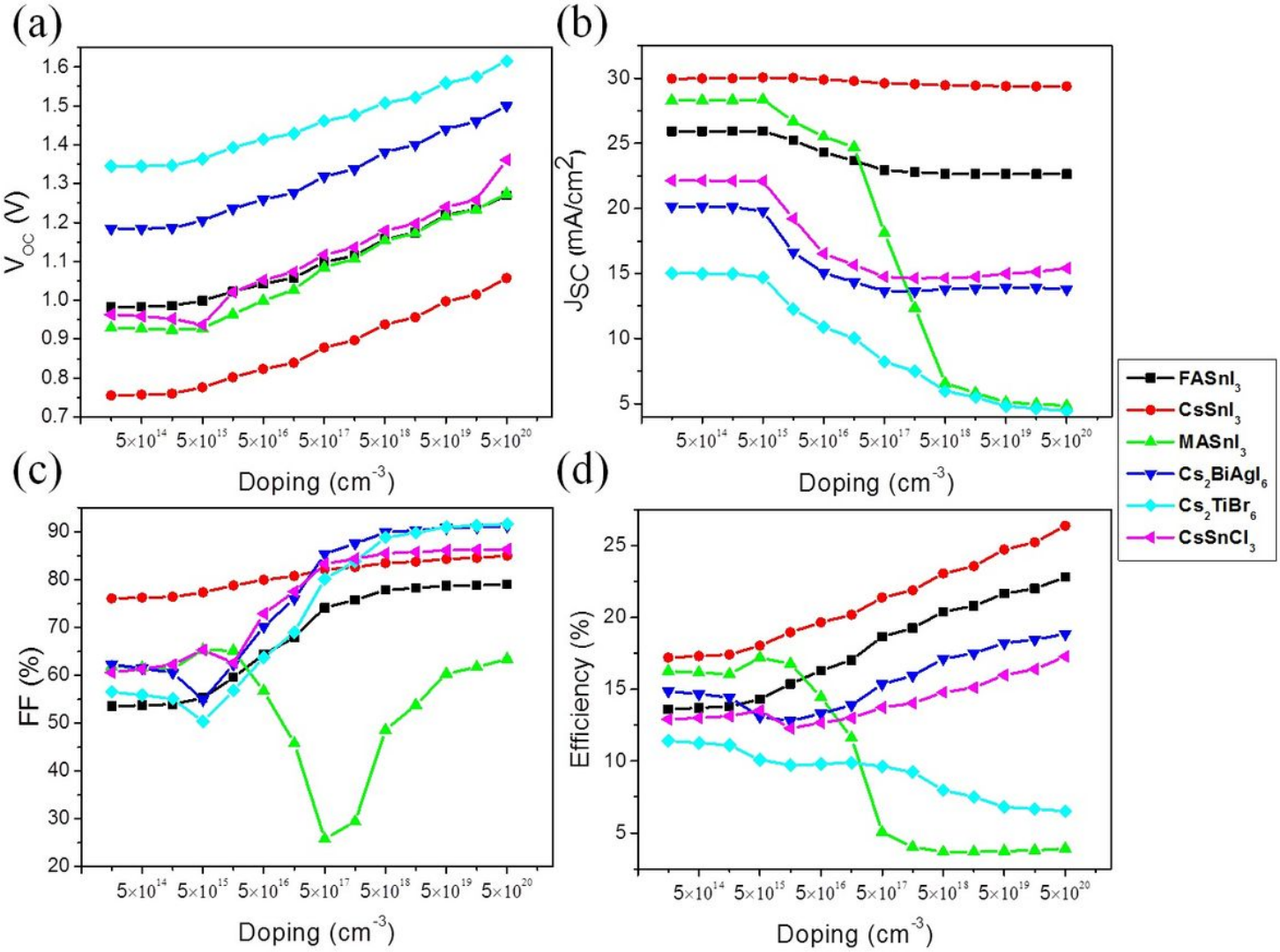

Figure 3

Impact of doping variation on the performance parameters of Pb-free perovskites

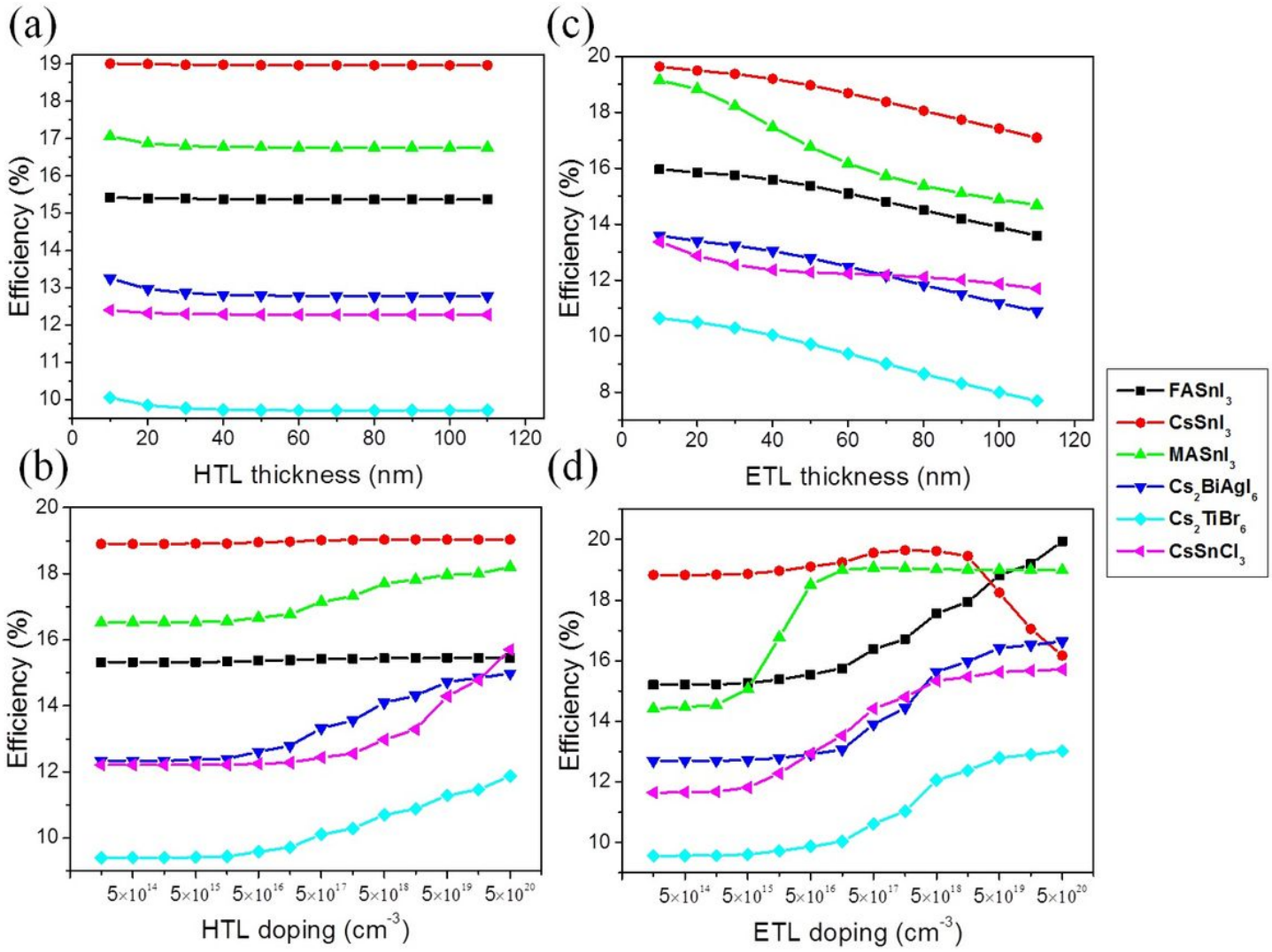

Figure 4

Impact of doping and thickness variation of ETL, HTL on PSC performance

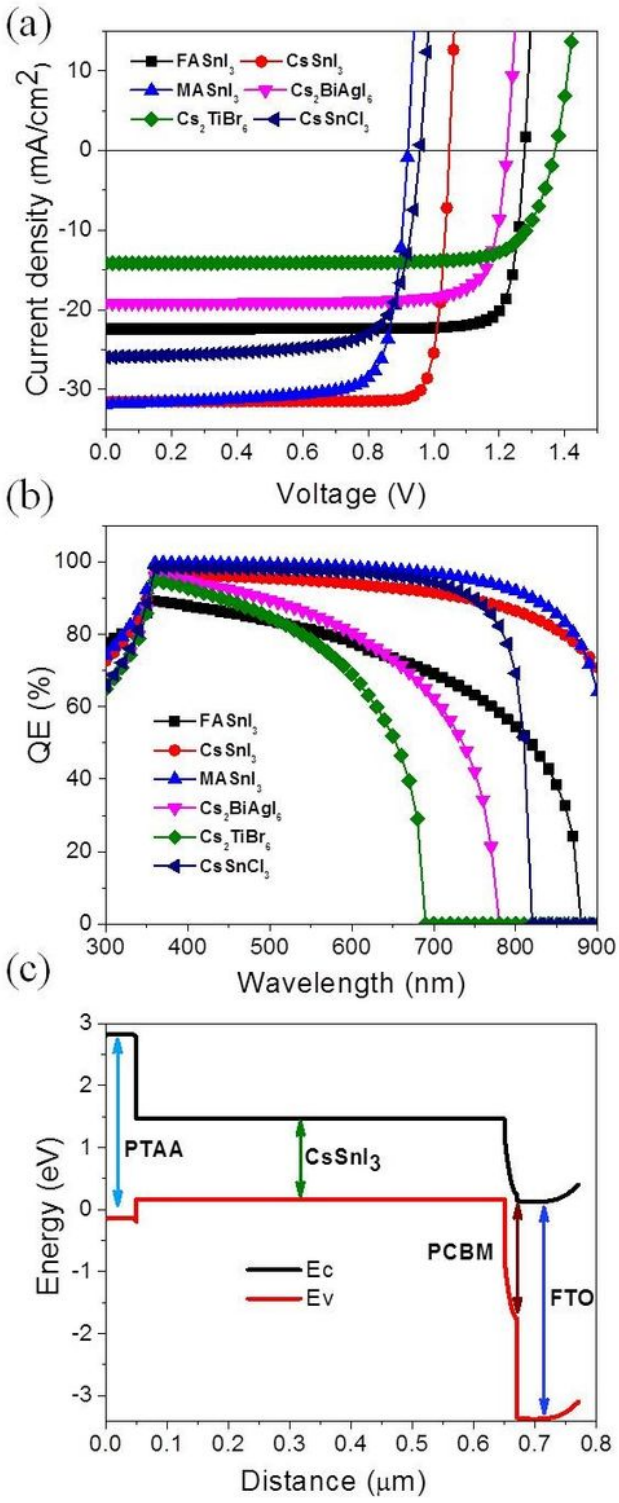

Figure 5

(a) J-V characteristics, and (b) corresponding QE spectra of PSCs with different Pb- free perovskites. (c) Energy band structure diagram of the CsSnI3 based perovskite solar cell.